MEMOIR OF THE GEOLOGICAL SOCIETY OF CHINA
NO. 4, PP 67-89, 12 FIGS. OCTOBER 1981

MECHANICS OF MOUNTAIN BUILDING AND METAMORPHISM IN TAIWAN

JOHN SUPPE[1]

ABSTRACT

The Philippine Sea plate is moving toward the northwest relative to the Asian plate at about 70 km/m. y. (Seno, 1977). This motion results in an oblique collision of the Luzon volcanic island arc with the Chinese continental margin, producing the island of Taiwan as a much expanded accretionary wedge composed largely of Cenozoic continental margin sediments. The rate of southward propagation of the collision with respect to the arc is about 90 km/m. y. Therefore, to a first approximation, to move 90 km south in the arc or in Taiwan is equivalent to moving 1 m. y. back in time. Using this time-space equivalence, by moving north from the southern tip of Taiwan we see that the accretionary wedge (Central Mountains) grows above sea level until the rate of material influx by orogenesis is balanced by the outflux by denudation. A steady-state mountain belt is attained in about 1 1/3 m. y., with a width of about 90 km and a cross-sectional flux of about 500 km^2/m. y.

Compression within the mountain belt is dominated by slip on thrust faults and related fault-bend folding within a wedge-shaped zone above a basal decollement. Based on construction of a regional retrodeformable cross section, the thrust-related shortening of the Chinese continental margin is not less than 150-200 km in northern Taiwan. The major horizons of decollement within the western foothills lie within zones of excess pore-fluid pressure (approximately 1.7 times hydrostatic), resulting in moderately low frictional resistance. The overall mechanics of the mountain wedge may be approximated as a wedge of Coulomb material at compressive failure throughout, analogous to the wedge of soil that develops in front of a bulldozer, which deforms until the critical stable surface slope α is attained. The critical taper at some point in the wedge with thickness h is (Davis and Suppe, 1980):

$$(\alpha+\beta)=\tan^{-1}\left[\frac{(1-\lambda_f)(\sin\beta+\mu_f)}{\{\lambda_0+K_p(1-\lambda_0)\}+\{C_0(K_p-1)/(\rho g h\tan\phi)\}}\right]$$

where α is the surface slope and β is the dip of the decollement. C_0, ϕ, $K_p=[(1+\sin\phi)/(1-\sin\phi)]$, and $\lambda_0=p_f/\rho g z$ are the cohesive strength, coefficient of internal friction, passive earth-pressure coefficient and Hubbert-Rubey fluid-pressure ratio within the wedge, respectively. λ_f and μ_f are the fluid-pressure ratio and coefficient of friction along the basal decollement. In western Taiwan we directly measure $\lambda_0=\lambda_f=0.7$, and $\beta=6°$. For $h<\backsim 4$km, $0<\alpha<3°$, and for $h>\backsim 4$km $\alpha=3°$. According to Byerlee's law $\mu_f=0.85$; thus we solve for $C_0\cong 5$

1 Department of Geological and Geophysical Sciences, Princeton University, Princeton, N Jersey 08544, U. S. A.

MPa and $\phi \cong 30°$, which is in excellent agreement with measured rock strengths of sedimentary rocks similar to those in western Taiwan. Therefore the deformed mountain wedge of western Taiwan has a shape in agreement with the theory of the Coulomb wedge.

The physical conditions of present-day regional metamorphism within the non-plastic zone (upper 10-13 km) implied by the regional shape of the mountain mass, involve solid overpressures (thermodynamic solid pressure or mean stress $\bar{\sigma}=1.3\ \rho gz$) and low fluid pressure-solid pressure ratio ($P_f/\bar{\sigma}=0.5$). In contrast, the mean stress of the Chinese continental margin prior to plate collision is estimated at $\bar{\sigma}=0.9\ \rho gz$ with a higher fluid pressure-solid pressure ratio $P_f/\bar{\sigma}=0.8$. The drop in fluid pressure-solid pressure ratio as a result of plate-collision is proposed as a significant cause of regional metamorphism at depths less than approximately 15 km in Taiwan. Temperature gradients in the western foothills are about 30-35°C/km based on petroleum exploration.

INTRODUCTION

Taiwan is the site of ongoing arc-continent collision between the Luzon volcanic arc at the west edge of the Philippine Sea plate and the Chinese continental margin (Fig. 1). This paper considers five aspects of the arc-continent collision:

1) Plate motions and kinematics of propagation of the collision with respect to the Luzon arc and the Chinese continental margin, including a time-space equivalence within the mountain belt.

1) Development of a steady-state mountain belt in central Taiwan in which the rate of mountain growth by plate compression is balanced by the rate of erosion.

3) Role of thrust imbrication and fault-bend folding in deformation within the mountain belt.

4) Critical cross-sectional taper of the Taiwan mountain belt in light of the wedge theory of compressive mountain belts.

5) The predicted present-day physical conditions of metamorphism within the Taiwan mountain belt based on the wedge theory and the change in conditions in the continental margin as a result of arc-continent collision.

To the east and northeast of northern Taiwan, the Philippine Sea plate is subducting northward beneath the Ryukyu Trench. In contrast, from Taiwan south to Luzon, the Philippine Sea plate is overriding lithosphere of the Asian plate along the Manila Trench and its northern continuation, the foredeep of western Taiwan. As we proceed from south to north along the plate boundary, it impinges in turn on the abyssal plain of the South China Sea and then the Chinese continental rise, slope, and shelf (Fig. 1).

There is considerable morphotectonic continuity between Taiwan and the Luzon arc to the south. The Luzon volcanic arc, including the islands of Babuyan, Batan, Lanyu, and Lutao (Fig. 1), continues northward into the low Coastal Range of eastern Taiwan where Neogene island-arc volcanic rocks are exposed

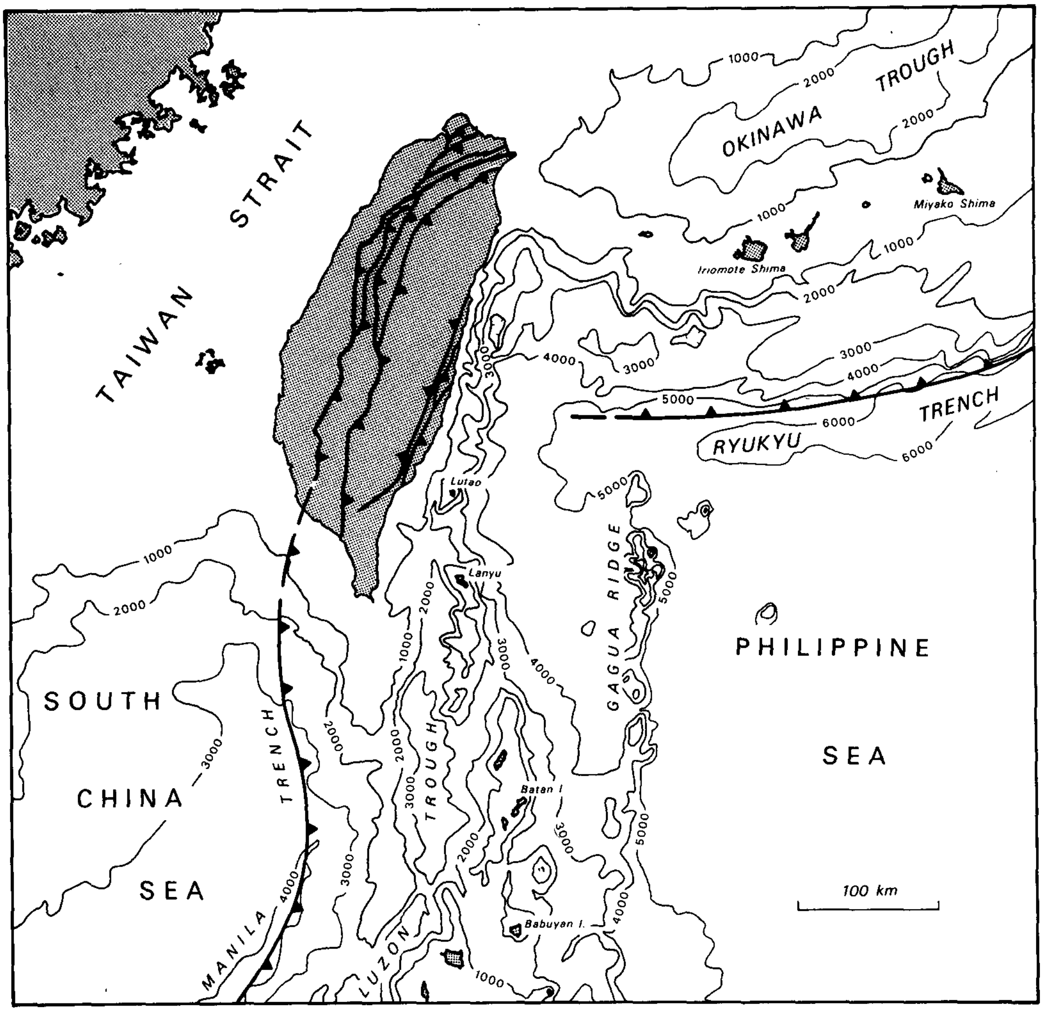

Fig. 1. Bathymetry and tectonic setting of Taiwan region (after Suppe, 1980a).

(Ho, 1979). The submerged outer non-volcanic arc (accretionary wedge) expands continuously toward the north, rising above sea level to merge morphologically with the great Central Mountains of Taiwan (Figs. 1 and 2), which are constructed of west-vergent thrust sheets as discussed below.

The intervening Luzon Trough, a forearc basin, narrows and shallows towards the north and projects directly into the southern Coastal Range and into the Longitudinal Valley between the Coastal Range and the Central Mountains (Fig. 2). The Coastal Range contains uplifted and deformed sediments of the Luzon Trough as well as of the Luzon volcanic arc (Page and Suppe, 1981; Chi *et al.*, 1981).

KINEMATICS OF ARC-CONTINENT COLLISION

According to Seno (1977) the present-day rate of plate convergence near

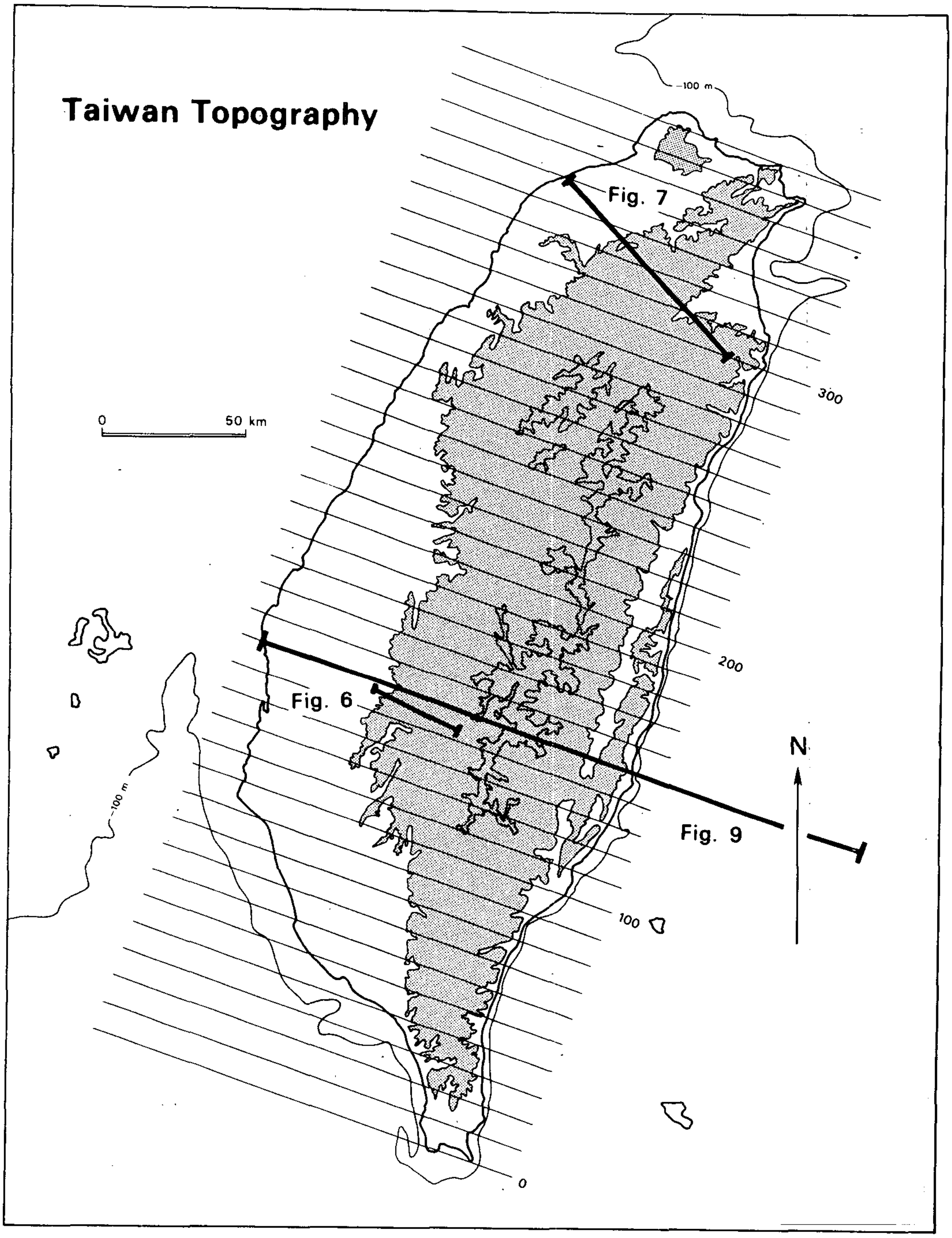

Fig. 2. Simplified topography of Central Mountains of Taiwan. Area above 200 m in screened pattern; higher contour is 2000 m. Family of straight lines show locations of topographic profiles in Fig. 4. Profiles are labeled in distance in kilometers N 20°E of southern tip of Taiwan.

Taiwan is about 70 km/m.y. in a northwest-southeast direction ($\omega = 1.2°$/m.y., 45.5°N, 150.2°E). The collision is oblique because the stable continental shelf of China is oriented northeast-southwest (Fig. 1) whereas the Luzon island arc is oriented north-south. The collision is just now beginning in southernmost Taiwan whereas it began 4 m.y. ago in northern Taiwan based on stratigraphic studies (Chi *et al.*, 1981).

Let us consider the geometry of collision in more detail (Figs. 1 and 3). The overall rate of plate compression in Taiwan is about 70 km/m.y. (7 cm/y) in a N 55°W direction. The arc is oriented about N 16°E whereas the continental margin is oriented N 60°E. Therefore the angle between the arc and the compression is about 71°; and the angle between the continental margin and the compression is about 65° (Fig. 3). We may solve for the rate of propagation of the collision with respect to the arc of 90 km/m.y. and with respect to the continental margin of 95 km/m.y., as shown in Fig. 3.

Both the island arc and the stable continental margin have a cylindrical symmetry to the first approximation, therefore their collision should be similar at each point in time, only shifted in space. This time-space equivalence provides a powerful tool for tectonic analysis. To move 90 kilometers south along the arc is equivalent to moving 1 m.y. back in time. Page and Suppe (1981) used this equivalence to help analyze the paleogeography of the Upper Pliocene Lichi Melange of the southern Coastal Range of eastern Taiwan. An area 180 to 250 km

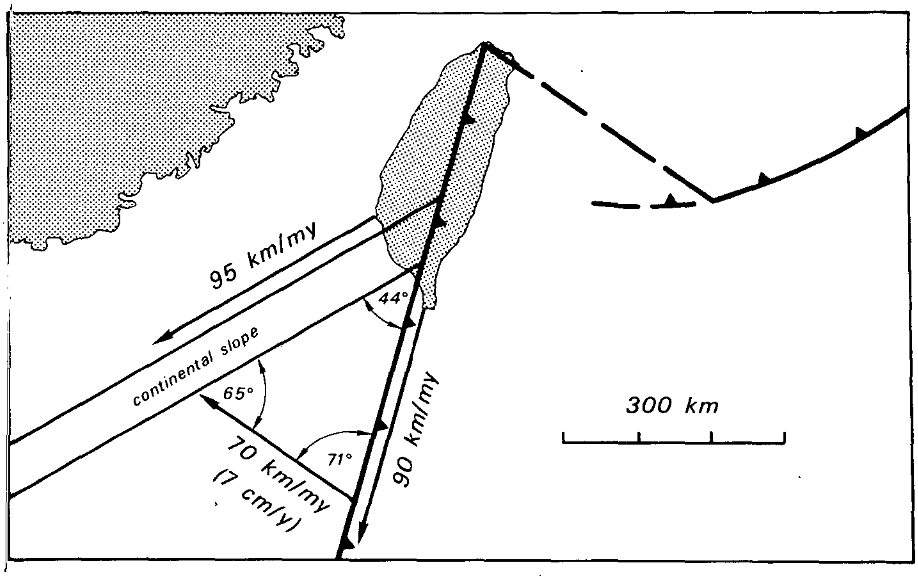

Fig. 3. Velocity triangle for arc-continent collision. Given the plate convergence of 70 km/m.y. (Seno, 1977) and the angle between the continental slope and arc of 44° we determine that the collision propagates south along the arc at about 90 km/m.y. and southwest along the continental margin at about 95 km/m.y.

to the south along the arc in the Luzon Trough (Fig. 1) has a bathymetry in close agreement with that deduced from sedimentologic studies of the Lichi Melange. In the following section we make further use of the time-space equivalence.

STEADY-STATE TOPOGRAPHY OF TAIWAN

The major bathymetric and topographic effect of the arc-continent collision is the expansion of the accretionary wedge (outer non-volcanic arc) in both width and height as the plate boundary encounters and incorporates the thick sediments of the Chinese continental rise, slope, and shelf (Fig. 1). More than 150 kms south of Taiwan, the accretionary wedge is about 50 km wide with a crest 1500 to 2000 m below sea level. In the region 0 to 150 kms south of Taiwan, the accretionary wedge expands to double this width as it encounters the Chinese continental rise and slope (Fig. 1). With continued arc-continent collision the accretionary wedge rises above sea level to become the Central Mountains of Taiwan (Fig. 2).

We can observe the growth of the mountain belt in time by moving north from the southern tip of Taiwan, using the time-space equivalence discussed in the previous section. The mountains grow steadily wider and higher (Figs. 2 and 4) until at about 120 kms north (1⅓ m. y.) there is a constant width of $87 \pm 4\,(2\sigma)$ kms, a cross sectional area of $118 \pm 24\,\mathrm{km}^2$, and a mean elevation of 1350 meters. The constant mountain size continues to about 290 kms north of the southern tip, beyond which the topography becomes rapidly subdued, as discussed later.

Application of the time-space equivalence leads to the conclusion that the region of constant topography in central Taiwan (120 to 290 km north) is a region of steady-state topography in which the rate of growth of the mountain belt as a result of plate-boundary compression is equal to the rate of erosion. This observation implies that erosion places an upper limit to the size of this mountain belt and that this maximum size is reached in about 1⅓ m. y. (120 km north of southern tip of Taiwan, Fig. 5).

We may attempt to test the steady-state prediction because the rate of plate convergence (70 km/m. y.) and the erosion rate ($\sim$ 5.5 km/m. y.) are known in Taiwan (Seno, 1977; Li, 1976). The cross-sectional erosive flux $\dot{E}$ is the product of the erosion rate $\dot{d}$ and the mountain width w

$$\dot{E} = \dot{d}\,w\,, \tag{1}$$

which is about $480\,\mathrm{km}^2/\mathrm{m.y.}$ in central Taiwan (Fig. 5). The cross-sectional compressive flux $\dot{C}$ is more complex; in the simplest model it is the product of plate convergence $\dot{v}$ and the effective thickness t' of material compressed

$$\dot{C} = \dot{v}\,t'\,. \tag{2}$$

The effective thickness t' will be a true thickness t of material entering the mountain belt after correction for isostatic effects.

In the steady-state case we may ignore isostatic effects because there is no change in mass within the mountain and t' becomes t. Equating (1) and (2) we obtain the condition for a steady state mountain belt

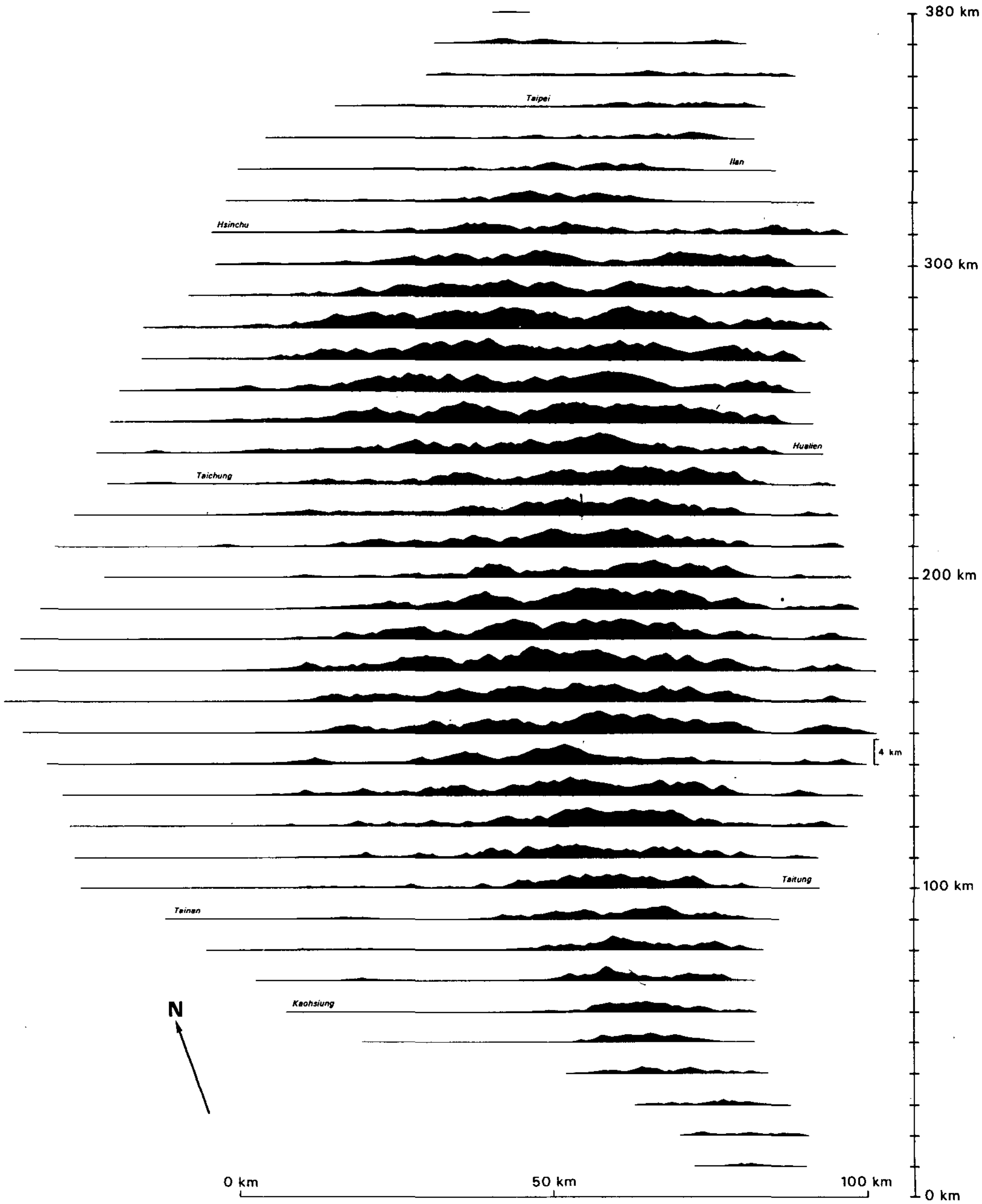

Fig. 4. Topographic profiles of Taiwan along the lines shown in Fig. 2 horizontal scale=vertical scale. Area above sea level shown in black.

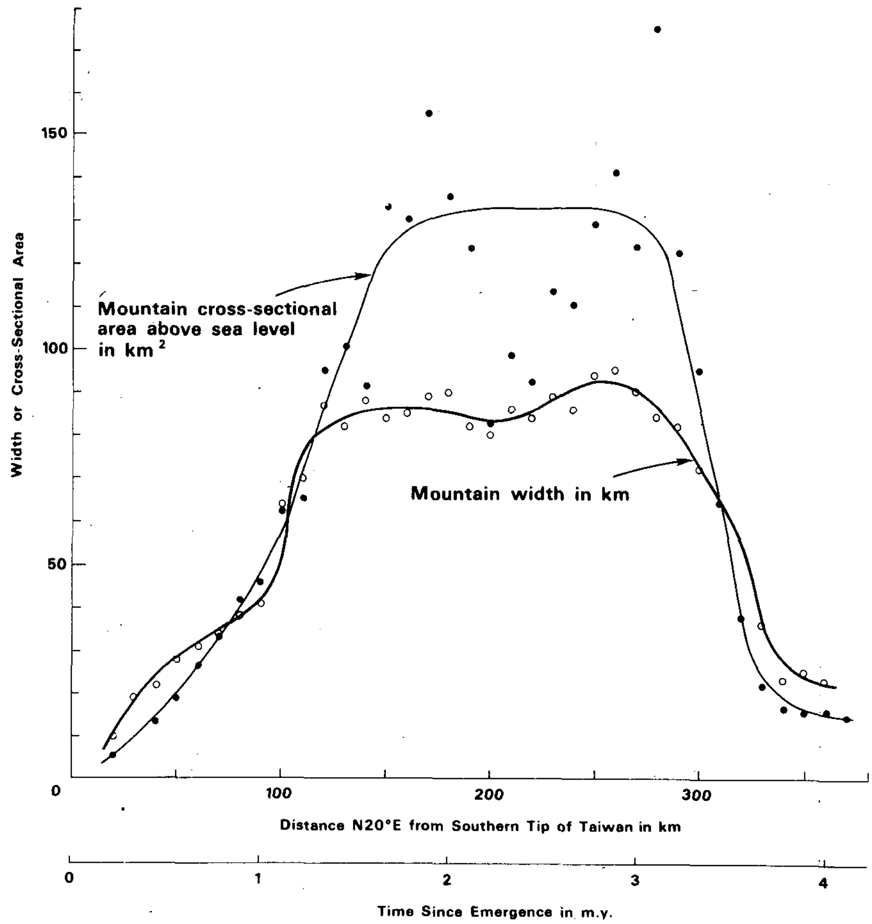

Fig. 5. Graph showing the width of the mountains of Taiwan (above 200 m) and cross-sectional area above sea level along the lines shown in Figs. 2 and 4. The horizontal scale shows the distance of the cross-section line from the southern tip of Taiwan and the time since emergence above sea level, assuming the time-space equivalence of Fig. 3.

$$t = \frac{\dot{d}w}{\dot{v}} . \qquad (3)$$

The thickness t required for a mountain belt of the width of central Taiwan (85 to 90 km) is about 7 kilometers. This result is in good agreement with the thickness of sediments entering the mountain belt in western Taiwan (see Figs. 6 and 7). Therefore we conclude that the topography in central Taiwan is close to steady state with a cross-sectional flux of about 480 km^2/m. y. This cross-sectional flux per million years is a factor of 3 larger than the cross-sectional area of the mountain belt above sea level (Fig. 5). Therefore the present shape of the mountain belt should closely reflect current tectonic conditions, a conclusion that is supported by studies of the regional surface slope discussed later in this paper.

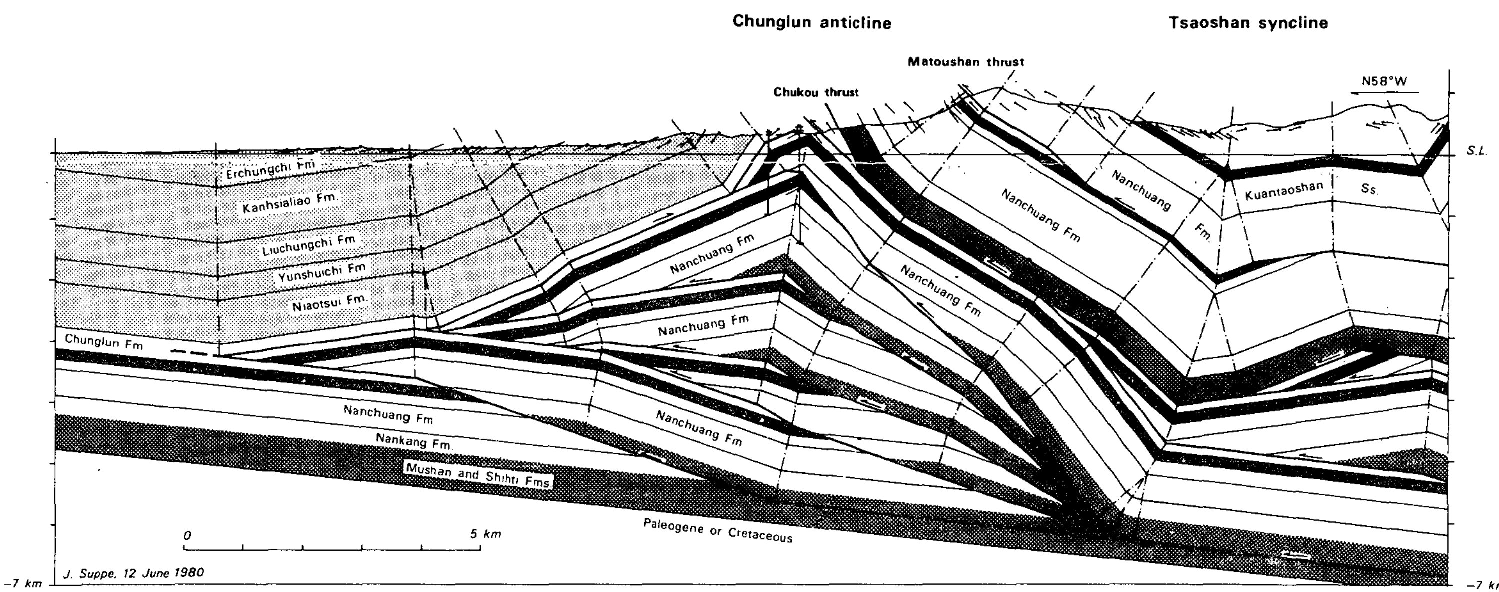

Fig. 6. Geologic cross section of western foothills of southern Taiwan through the Chunglun anticline (after Suppe, 1980b). The western edge of the cross section appears to be the western limit of important compressive deformation. Location of cross section shown in Fig. 2.

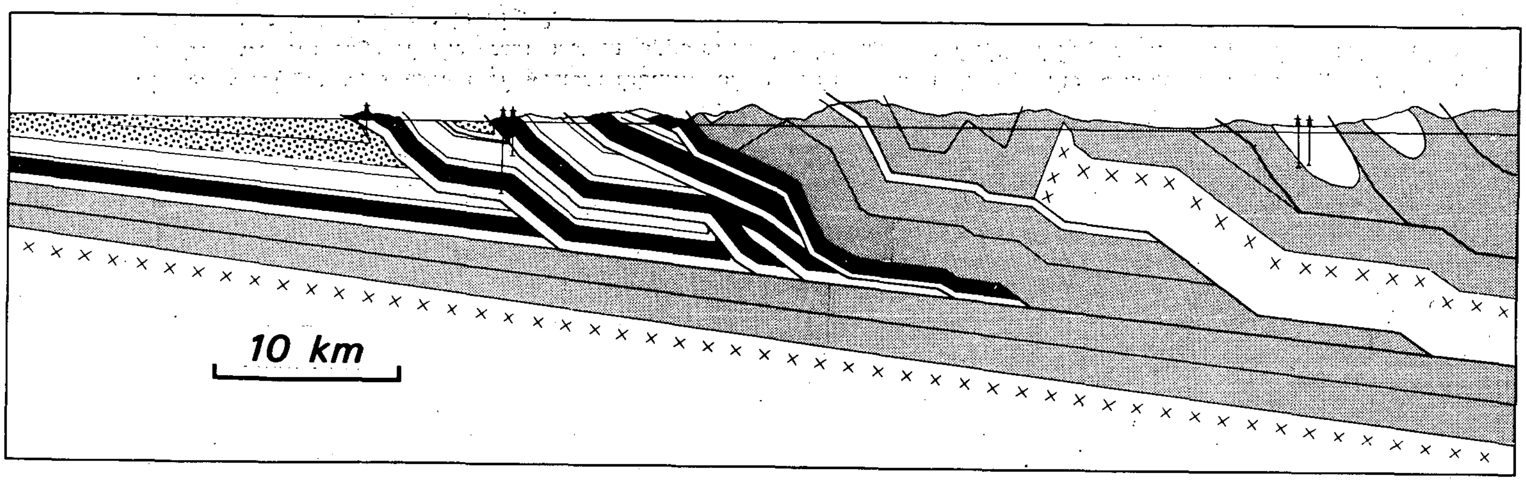

Fig. 7. Simplified structural cross section of northern Taiwan (after Suppe, 1980a). Location of cross section shown in Fig. 2.

If the mountain belt is at close to steady state, the rate of uplift should balance the rate of erosion, which is about 5.5 km/m. y. (Li, 1976). Peng *et al.* (1977) report uplift rates since the early Holocene of about 5.0 km/m. y., except in northern Taiwan where they are much less.

The subdued topography of northern Taiwan apparently reflects a reduced compressive flux, as discussed further below.

INTERNAL STRUCTURE

In the other sections of this paper we are concerned only with the overall shape of the Taiwan mountain belt. In this section we briefly describe the internal structure of the deformed rocks of the mountain belt, primarily to establish 1) the large horizontal compressive shortening and 2) the dip of the basal decollement. These two facts are important to the later discussion.

The structural geology of the Taiwan mountain belt is best mapped and studied in the western foothills were there has been extensive exploration for petroleum and coal (for example, Chinese Petroleum Corporation, 1971, 1974, 1978; Ho, 1975) and in the eastern Coastal Range (Hsu, 1956, 1976). These areas show large horizontal compression taken up mostly by slip on imbricate thrust faults (Suppe, 1980a, b; Suppe and Namson, 1979; Chi *et al.*, 1981). Figure 6 is an example of this strongly imbricate structure in the Chunglun area of southern Taiwan. Other cross sections of the foreland in western Taiwan are given by Suppe (1980a, b) and Suppe and Namson (1979). It is important to note that only the upper stratigraphic units of the Taiwan foreland are involved in these structures. The structure is detached from the deeper levels of the crust along a bedding-plane decollement, which dips about 6 degrees eastward under the mountain belt. The major horizons of decollement lie within zones of excess pore-fluid pressure ($\lambda = \sim 0.7$) resulting in moderately low frictional resistance (Suppe and Wittke, 1977; Pytte, 1980). The folding is a result of the bending of the thrust sheets as they ride over steps in decollement (fault-bend folding) (Suppe, 1979; Suppe Suppe and Namson, 1979).

The more interior parts of the Taiwan mountain belt also show large horizontal shortening. Fig. 7 is a retrodeformable cross section of north Taiwan, simplified from Suppe (1980a), in which a section presently 60 km wide had an original width of 180 km. The Plio-Pleistocene shortening of the Chinese continental margin in northern Taiwan was estimated by Suppe to be not less than 160 to 200 km based on the observed structures. Detailed mapping throughout the Central Mountains show large horizontal compression (for example, Ho, 1979; Wang-Lee and Wang, 1981; Chen, 1979; Stanley, 1981).

WEDGE SHAPE OF MOUNTAIN BELT

The structure of western Taiwan is similar to most compressive mountain belts in that it displays large horizontal compressive strain within a wedge-shaped mass ovelying a decollement as documented above. This property of mountain

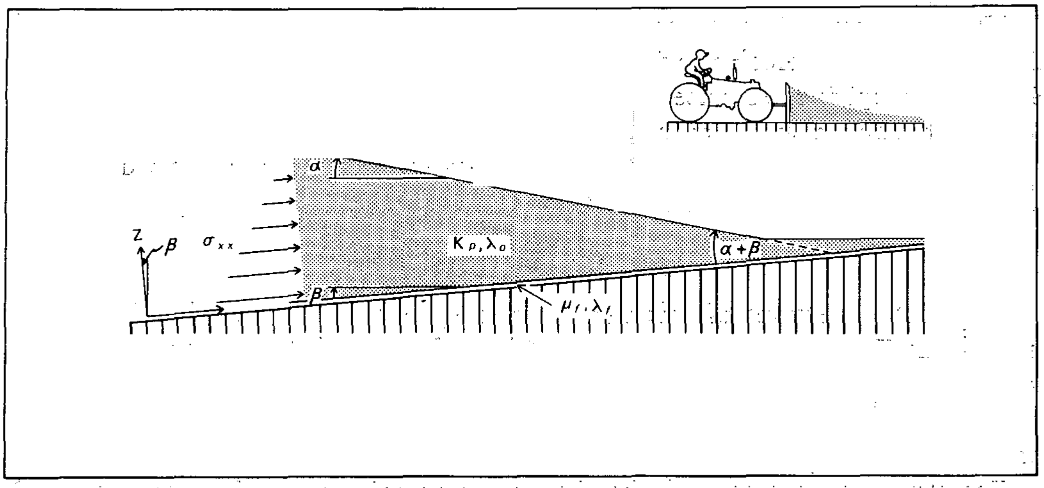

Fig. 8. Schematic wedge of Coulomb material at failure throughout by horizontal compression. The taper of the wedge is a function of the ratio of the friction along the base to the strength within the wedge (equation 6) (after Davis and Suppe, in preparation).

belts has given rise to the notion that their mechanics is similar to the wedge of soil or snow in front of a bulldozer (Chapple, 1978; Davis and Suppe, 1980) (Fig. 8). The soil deforms, increasing the surface slope until a critical taper is attained. Once the critical taper is established the wedge slides stably without changing shape, only growing in size if additional material is encountered.

The critical taper is the shape for which the strength of the material within the wedge is balanced by the resistance along the basal decollement (Fig. 8) (Chapple, 1978; Davis and Suppe, 1980). In the upper non-plastic part of the lithosphere, Coulomb behavior is appropriate (for example, Brace and Kohlstedt, 1980); for fracture we have

$$\sigma_\tau = C_0 + (\sigma_n - P_f) \tan\phi, \qquad (4)$$

and for friction

$$\sigma_\tau = T_0 + (\sigma_n - P_f)\,\mu_f, \qquad (5)$$

where σ_τ and σ_n are the shear and normal stresses on the surface at failure, P_f is the fluid pressure, C_0 and T_0 are cohessive strengths, ϕ is the angle of internal friction, and μ_f is the coefficient of static friction. Davis and Suppe (1980, in preparation) have derived the equation for the critical taper of a wedge of Coulomb material at failure by horizontal compression. We assume that an active mountain belt such as Taiwan has a state of stress everywhere at failure because the rocks are everywhere recently deformed and deformation continues throughout based on earthquake studies (Tsai *et al.*, 1977). Therefore the state of stress everywhere within the wedge is considered by Davis and Suppe (in preparation) to be defined by an equation of the form of equations 4 and 5. A comparison of the results of this assumption with the Taiwan mountain belt is used as a test. The rate of change of horizontal compressive force within the wedge is directly related to the rate of change in thickness of the wedge and is equal to the rate of change of the frictional force. Based on these considerations Davis and Suppe (1980, in preparation) obtain an expression for the critical taper, which when simplified to the subaerial case is

$$(\alpha+\beta)=\tan^{-1}\left[\frac{(1-\lambda_f)(\sin\beta+\mu_f)}{\{\lambda_0+K_p(1-\lambda_0)\}+\{C_0(K_p-1)/(\bar{\rho}gh\tan\phi)\}}\right], \quad (6)$$

where α is the surface slope and β is the dip of the decollement. C_0, ϕ, $K_p = \{(1+\sin\phi)/(1-\sin\phi)\}$, and $\lambda_0 = p_f/\bar{\rho}gz$ are the cohesive strength, coefficient of internal friction, passive earth-pressure coefficient and Hubbert-Rubey fluid-pressure ratio within the wedge, respectively. λ_f and μ_f are the fluid-pressure ratio and coefficient of friction along the basal decollement. We note from equation (6) that the taper $(\alpha+\beta)$ is essentially the ratio of friction along the base to strength within the wedge; friction increases the taper whereas strength decreases it. Furthermore as the wedge becomes large (thickness h becomes large) the taper becomes constant and independent of cohesion and gravity.

Davis and Suppe (1980, in preparation) have applied the Coulomb-wedge theory to western Taiwan. The mean surface slope for profiles 100 through 240 in Fig. 4 is $\alpha = 2.9° \pm 0.3°(2\sigma)$ for $h > 4$ km and for $h < 4$ km $0 < \alpha < 2.9°$. The dip of the basal decollement is known in central Taiwan from well and seismic data in the foreland and construction of retrodeformable cross sections in the fold-and-thrust belt such as Fig. 6, $\beta = 6°$ $(\pm \sim 0.5°)$. Fluid-pressures are known from formation tests and sonic-log data in the foothills, $\lambda_0 = \lambda_f = 0.7$ (Suppe and Wittke, 1977; Pytte, 1980; Suppe, Namson and Pytte, in preparation). The only parameters in equation (6) that are not directly measured in western Taiwan are K_p (or ϕ), C_0, and μ_f. Coefficients of friction μ_f for rocks at geologic confining pressures are essentially constant for nearly all rock types, $\mu_f = 0.85$ (Byerlee, 1978). Therefore we solve for $C_0 \leq 5$ MPa (50 bars) and $25° \leq \phi \leq 30°$ which are the most typical laboratory values for strengths of rocks such as those in Taiwan (Clark, 1966; Hoshino *et al.*, 1972). Therefore, we conclude that the fold-and-thrust belt of central western Taiwan has a shape in very close agreement with equation (6). Therefore, given the high rate of erosion (Li, 1976) the mountain belt continuously deforms, adjusting itself to the critical profile.

The region of subdued topography in northern Taiwan has a very low and irregular regional surface slope (Figs., 2, 4, 5, and 7). We therefore conclude that the mountain belt in northern Taiwan is no longer at failure throughout and has ceased active deformation, as is evidenced by earthquake seismic data (Tsai *et al.*, 1977) and the onlap of underformed later arc-volcanic rocks of the Ryukyu chain in northernmost Taiwan (Ho *et al.*, 1963; Ho *et al.*, 1964; Bojo *et al.*, undated; Ku *et al.*, 1963).

Fig. 9 is a regional cross section through southern Taiwan near the area of

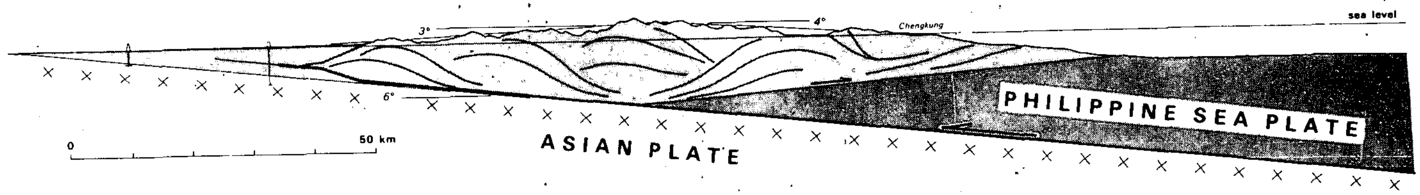

Fig. 9. Regional tectonic cross section of Taiwan along line 150 of Figs. 2 and 4. The cross section shows the deformation within the mountain belt only schematically (see Figs. 6 and 7 and Stanley *et al.*, 1981 for more detail). The dip of the decollement under eastern Taiwan was computed as discussed in the text.

Fig. 6 with the interior deformed structure of the mountain belt only shown schematically. The dip of the basal east-dipping decollement is 6° as discussed above. At the crest of the mountain belt the surface slope reverses and dips to the east at $\alpha = -4°$ in the subaerial part. We compute the dip of the decollement under eastern Taiwan subaerial mountain belt to be $\beta = -4.5°$ assuming the same rock conditions as western Taiwan. For continuity of displacement we choose the two decollement to coincide under the crest of the mountain belt (Fig. 9) and project the eastern decollement to the east where it interesects the sea bottom at the foot of the continental slope, which is also the eastern limit of shallow seismicity (Tsai *et al.*, 1977). Therefore we conclude tentatively that a double-sided wedge exists in Taiwan. The analysis of the underwater surface slope α offshore eastern Taiwan is beyond the domain of equation (6) and the scope of this paper but agrees qualitatively with the more general underwater equation (Davis and Suppe, in preparation).

CONDITIONS OF METAMORPHISM IN RELATION TO THE SHAPE OF THE MOUNTAIN BELT

The shape of the compressive mountain belt in Taiwan, which was just discussed, has important implications for the conditions of present-day metamorphism within the mountain belt and for our understanding of the origin of regional low-grade metamorphism. By low-grade metamorphism we mean metamorphism at or above the brittle-plastic transition, where rocks have their highest strength. For quartz-rich rocks this transition may be typically in the depth range 15-20 km (e. g. Brace and Kohlstedt, 1980). In light of the Coulomb-wedge analysis given above and the thickness of the mountain belt (Fig. 9) Taiwan is apparently at or above the brittle-plastic transition above the basal decollement.

The important physical variables controlling the stability of mineral assemblages are considered to be temperature T, solid pressure P_s, and fluid pressure P_f. The composition of the fluid is of course important to the mineral assemblage, but is beyond the scope of this discussion (see Liou, 1981), and may be buffered by the assemblage of solid phases. The thermodynamic solid pressure P_s in general is the mean stress $\bar{\sigma}$

$$P_s = \bar{\sigma} = \left[\frac{\sigma_1 + \sigma_2 + \sigma_3}{3}\right], \qquad (7)$$

where σ_1, σ_2, σ_3 are the principal stresses. It is sometimes assumed in metamorphic petrology that the state of stress is isotropic and equal to the overburden pressure $\rho g z$

$$\bar{\sigma} = \sigma_1 = \sigma_2 = \sigma_3 = \rho g z\,, \qquad (8)$$

which is the assumption of *lithostatic stress*. The lithostatic assumption for Taiwan and other compressive mountain belts is in clear violation of the Coulomb-wedge analysis of the previous section as well as *in situ* stress measurements throughout the world (for example, McGarr and Gay, 1978). In this section we examine the effect of the nonisotropic state of stress on the mean stress in Taiwan and consider how that mean stress may have changed during the arc-continent collision.

It is also sometimes assumed in metamorphic petrology that fluid pressure is equal to solid overburden pressure

$$P_f = P_s = \rho g z \,. \tag{9}$$

This may be called the assumption of *lithostatic fluid pressure*, which in Taiwan is in violation of direct measurements in the western foothills (Suppe and Wittke, 1977; Pytte, 1980; Suppe, Namson and Pytte, in preparation) and of the Coulomb-wedge analysis. In this section we also examine the effects of non-lithostatic fluid pressure as well as nonisotropic stress on the conditions of metamorphism in Taiwan. The effects appear to be substantial. We proceed by deriving the equations for $\bar{\sigma}$ and $P_f/\bar{\sigma}$.

The state of stress in Taiwan was assumed to correspond to failure by horizontal compression in the Coulomb-wedge analysis; this state is described by the passive earth-pressure coefficient, ignoring $C_0 \sim 5$ MPa.

$$K_p = \left[\frac{\sigma^*_{horiz}}{\sigma^*_{vert}}\right] = \left[\frac{1 + \sin\phi}{1 - \sin\phi}\right], \tag{10}$$

where the starred stresses are effective normal stresses

$$\sigma^*_n = (\sigma_n - P_f) \,. \tag{11}$$

The vertical effective normal stress is just simply

$$\sigma^*_3 = \rho g z (1 - \lambda) \tag{12}$$

where $\lambda = P_f/\rho g z$ is the Hubbert-Rubey fluid-pressure ratio. From equation (10) we obtain the horizontal effective stress

$$\sigma^*_1 = \sigma^*_3 K_p = \rho g z K_p (1 - \lambda) \tag{13}$$

and

$$\sigma_1 = \rho g z [\lambda + K_p (1 - \lambda)] \,, \tag{14}$$

assuming for simplicity $\sigma_2 = \bar{\sigma}$,

$$\bar{\sigma} = \frac{\rho g z}{2} [1 + (\lambda + K_p (1 - \lambda))] \tag{15}$$

and

$$P_f/\bar{\sigma} = \frac{2\lambda}{[1 + (\lambda + K_p (1 - \lambda))]} \tag{16}$$

Before we proceed to the specific application of equations (15) and (16) to present-day metamorphism in Taiwan, it is appropriate to consider the state of the Chinese continental margin in Taiwan prior to the collision of the Luzon island arc. The best guess is that it was in a state of Coulomb failure by horizontal extension, which is described by the active earth-pressure coefficient

$$K_a = \left[\frac{\sigma^*_{horiz}}{\sigma^*_{vert}}\right] = \left[\frac{1 - \sin\phi}{1 + \sin\phi}\right] \tag{17}$$

which is the reciprocal of K_p (equation 10). A justification of equation (17) as a description of the state of stress in stable continental margins is the observation that this is the state of stress in the U. S. Gulf Coast continental margin (McGarr and Gay, 1978). The equations analogous to (15) and (16) for the "active" or extensional failure state differ only by a change of earth pressure coefficient

$$\bar{\sigma} = \frac{\rho g z}{2}\left[1 + (\lambda + K_a(1 - \lambda))\right] \tag{18}$$

and

$$P_f/\bar{\sigma} = \frac{2\lambda}{\left[1 + (\lambda + K_a(1 - \lambda))\right]}. \tag{19}$$

The mean stress in active or passive states of Coulomb failure differs substantially from $\rho g z$ if the fluid pressure is substantially less than the solid overburden ($\lambda < 1$). The most extreme case on the Earth corresponds to hydrostatic fluid pressures ($\lambda \sim 0.4$) and normal rock strengths ($\phi \sim 30°$, $K_p = 1/K_a \sim 3$). In this case

$$\left[\frac{\bar{\sigma}}{\rho g z}\right]_{active} = 0.8; \quad \left[\frac{\bar{\sigma}}{\rho g z}\right]_{passive} = 1.6\,.$$

Therefore, the mean stress or solid pressure doubles in changing from a stable continental margin to a compressive mountain belt with a hydrostatic fluid pressure. The effect is less in Taiwan with a more elevated fluid pressure ($\lambda \sim 0.7$) and an internal friction of $\phi \sim 30°$; in this case

$$\left[\frac{\bar{\sigma}}{\rho g z}\right]_{active} = 0.9; \quad \left[\frac{\bar{\sigma}}{\rho g z}\right]_{passive} = 1.3\,.$$

Therefore, we can expect about a 45% increase in mean stress as a result of the arc-continent collision in Taiwan. This result assumes no increase in fluid pressure as a result of the collision, but is an upper bound in any case. The state of stress and fluid pressure could be measured directly in the stable continental margin southwest of Taiwan (Fig. 1).

We now wish to compute the $P_s = \bar{\sigma}$ vs. T curves for Taiwan before and after the plate collision. Present-day thermal gradients measured in western Taiwan are about 30°C/km (for example, Suppe and Wittke, 1977). Assuming the steady-state heat flow equation to be valid for rocks just before they are incorporated into the fold-and-thrust belt, we have (Carslaw and Jaeger, 1959)

$$T = a + bz - \frac{A_0}{2K} z^2\,, \tag{20}$$

where a is the surface temperature (assumed to be 25°C), b is the gradient at the surface (taken to be 30°C/km), A_0 is the heat production (assumed to be 2.3×10^{-13} Cal cm^{-3} sec^{-1}; Wollenberg *et al.*, 1967), and K is the conductivity (about 6.5×10^{-3} Cal cm^{-1} sec^{-1} °C^{-1}; Clark, 1966).

Figure 10 presents the $\bar{\sigma} = P_s$ vs. T curves for Taiwan before (equation 18) and after collision (equation 15) with a lithostatic curve (equation 8) for comparison. Individual rocks undergo an adiabatic increase in solid pressure $\bar{\sigma}$ as a result of the change in state of stress during arc-continent collision.

Rocks in the foredeep both west and east of Taiwan undergo several kms of rapid sedimentary burial immediately preceding incorporation in the mountain belt at rates ranging from 3 to 10 km/m. y. (Chen *et al.*, 1977; Chi *et al.*, 1981). After entry into the mountain belt the rocks may be either uplifted or buried at rates of the order of 5 km/m. y. as a result of erosion and imbrication of thrust sheets. The effect of this rapid sedimentary or structural burial and rapid erosion on temperatures in the mountain belt can be treated as a moving-boundary heat flow problem (e. g. Clark and Jager, 1969; Alberede, 1976) but is beyond the scope of this paper. Here we are concerned only with the effects of the state of stress on metamorphism in Taiwan.

Plate collision appears to have very substantial effects on $P_f/\bar{\sigma}$ which is of critical importance in dehydration and decarbonation reactions. The value of

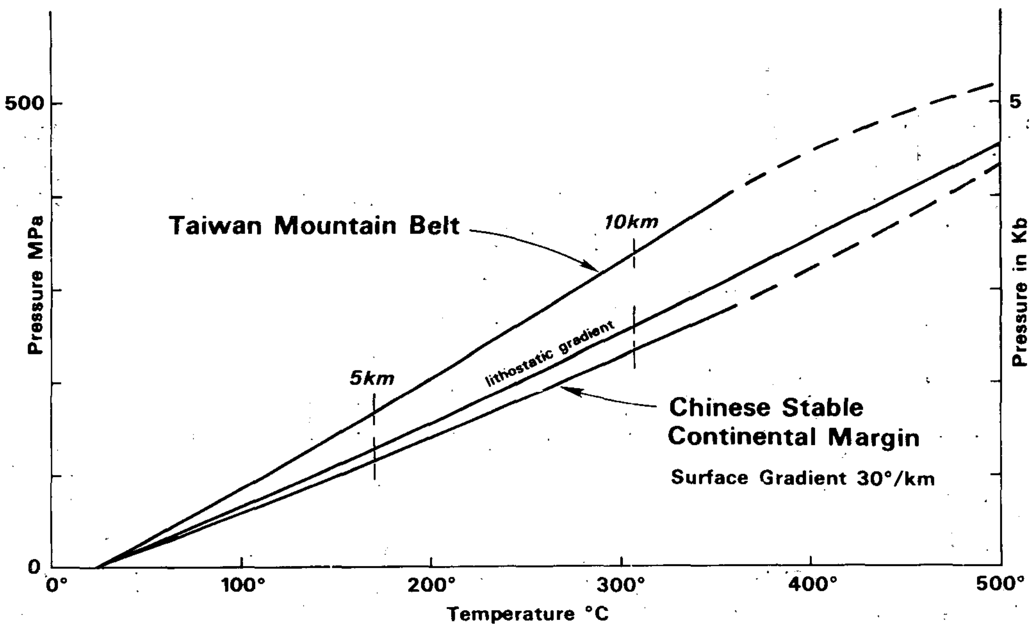

Fig. 10. Temperature-solid pressure curve for the Taiwan mountain belt assuming a surface gradient of 30°C/km and equations 15 and 20. The curves for a lithostatic gradient (equation 8) and a stable continental margin (equation 18) are shown for comparison.

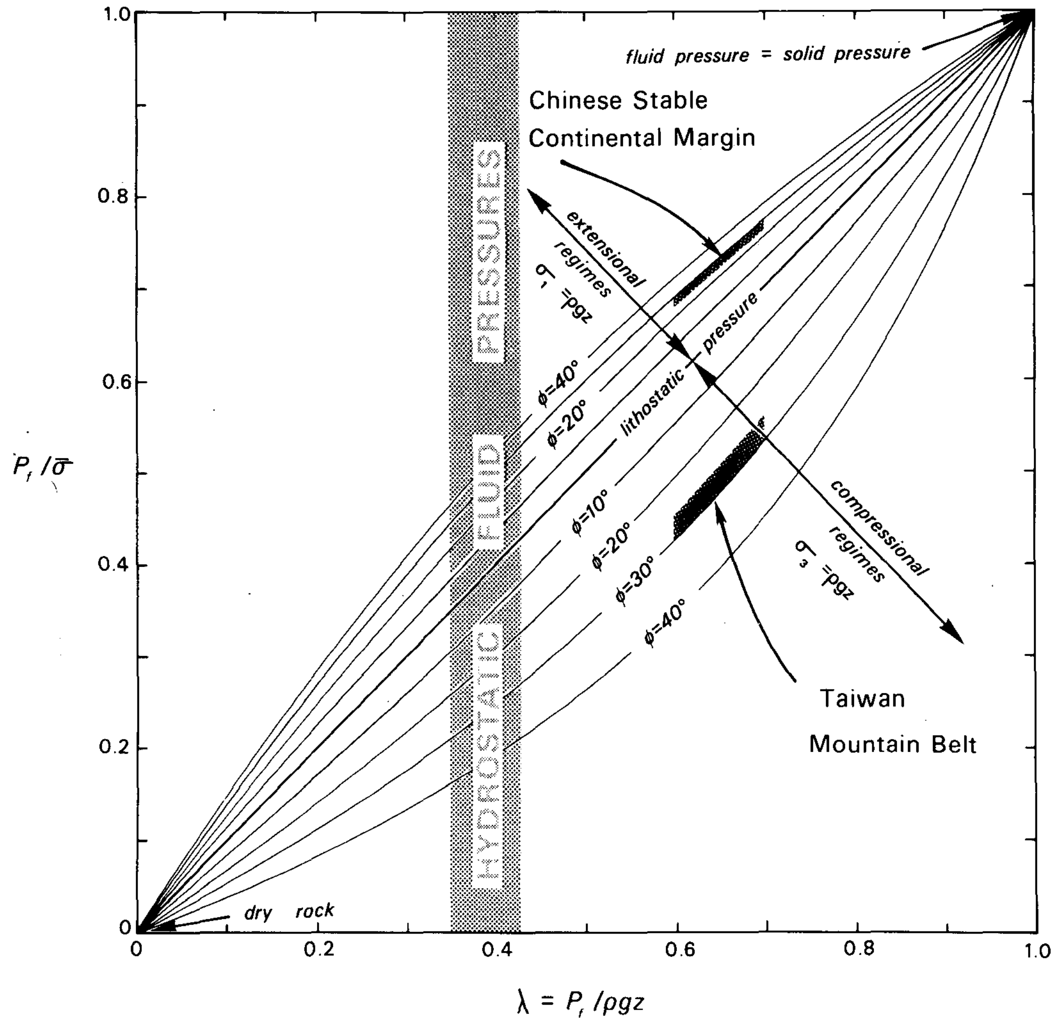

Fig. 11. Relationship between fluid pressure-solid pressure ratio $P_f/\bar{\sigma}$ and fluid-pressure ratio λ for extensional and compressional regimes (equations 16 and 19). The present-day conditions in Taiwan are shown. The conditions for the Chinese stable continental margin, assuming the same λ as Taiwan, are shown to illustrate the change in $P_f/\bar{\sigma}$ as a result of change in stress during arc-continent collision.

$P_f/\bar{\sigma}$ at active or passive failure is solely a function of ϕ and λ (equations 10, 16, 17, and 19). The solutions are graphed in Fig. 11. At constant rock strength ϕ the change in $P_f/\bar{\sigma}$ as a result of arc-continent collision is essentially constant for a wide range of fluid-pressure gradients λ. With typical strengths of $25° \leq \phi \leq 30°$ the change in $P_f/\bar{\sigma}$ is about 0.25. In the hydrostatic case ($\lambda = 0.4$)

$$\left[\frac{P_f}{\bar{\sigma}}\right]_{\text{extensional}} = 0.45; \left[\frac{P_f}{\bar{\sigma}}\right]_{\text{compressional}} = 0.2.$$

In the case of Taiwan ($\lambda = 0.7$) assuming as an upper bound that λ is unchanged during collision

$$\left[\frac{P_f}{\bar{\sigma}}\right]_{\text{extensional}} = 0.8; \quad \left[\frac{P_f}{\sigma}\right]_{\text{compressional}} = 0.55 .$$

The slope $d\bar{\sigma}/dT$ of a univarient reaction boundary is (Thompson, 1955)

$$\left[\frac{d\bar{\sigma}}{dT}\right]_{\Delta G=0} = \left\{\frac{\Delta S}{\Delta V_s + \Delta V_f[dP_f/d\bar{\sigma}]}\right\} \tag{21}$$

where ΔS, ΔG, ΔV_s, and ΔV_f are the changes in entropy, Gibbs free energy, and molar volumes of solids and fluids. Therefore the general petrologic effect of arc-continent collision is a steepening of the slopes ($d\bar{\sigma}/dT$) of univariant dehydration and decarbonation reaction boundaries, shifting them to lower temperatures (Fig. 12). Material particles, in contrast, move nearly adiabatically in response to the change in stress, as discussed above. The initial petrologic effect of arc-continent collision is therefore, to the first approximation, isothermal dehydration and decarbonation as a result of the increase in solid pressure $\bar{\sigma}$ with little change in fluid-pressure gradient λ. A more complete analysis requires considerations of specific reactions, permeabilities, and length scales. Nevertheless, a fundamental cause of the present-day metamorphism in the Central Mountains of Taiwan (Liou, 1981) is apparently change in stress.

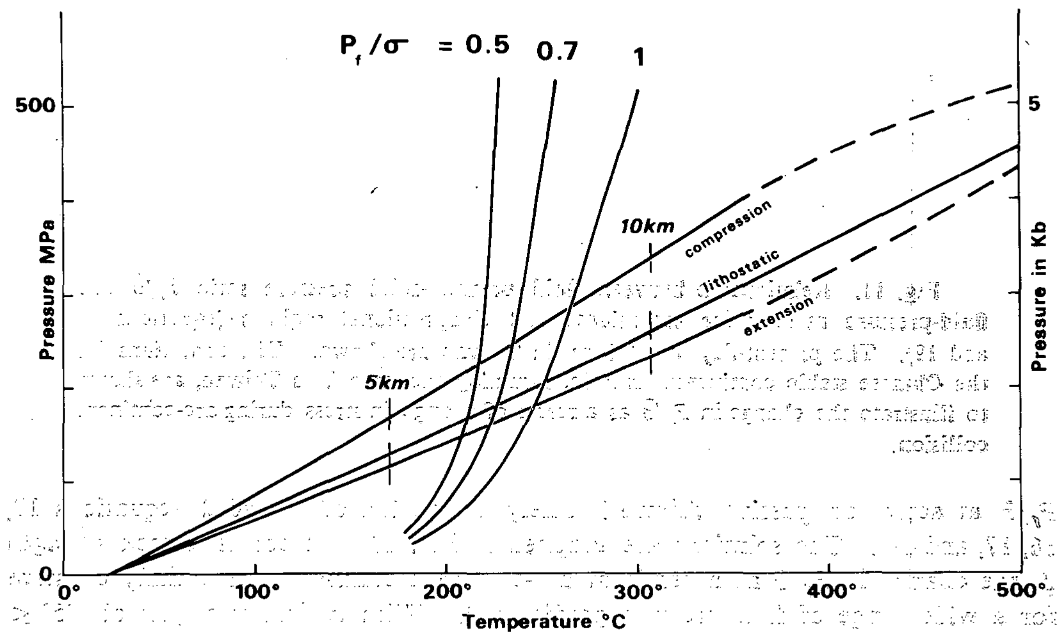

Fig. 12. Change in position of a typical dehydration reaction boundary as a result of change in stress during arc-continent collision (see Figs. 10 and 11 and equation 21). Rock particles may change from hydrated to dehydrated stability fields as a result of the change in stress.

ACKNOWLEDGEMENTS

I am grateful to many people and organizations for their contributions to my work in Taiwan. In the present study I am particularly grateful to J. Namson and J. Bialkowski for their help with the topographic studies and to Brian Evans for discussions on state of stress and material properties of the lithosphere. I thank the Taiwan Petroleum Exploration Division of the Chinese Petroleum Corporation for their hospitality and support of the work in the fold-and-thrust belt of Taiwan. This research is supported by the U. S. National Science Foundation grants EAR-7925446 and EAR-8018350. I am grateful to the John Simon Guggenheim Memorial Foundation for gracious and unencumbered support during 1978-1979. I thank W. G. Ernst and R. S. Stanley for their reviews.

REFERENCES

ALBEREDE, F. (1976) Thermal models of post-tectonic decompression as exemplified by the Haut-Allier granulites (Massif Central, France): *Bull. Soc. geol. France* **18**, 1023-1032.

BOJO, T., OTSU, H., WAN, S. M., YU, C. W. and WANG, M. C. (undated) Geologic and Topographic Map of Chinkuashih area: Mining Research and Service Organization, Taipei (Scale 1:10,000).

BYERLEE, J. (1978) Friction of rocks: *Pure and Applied Geophys.* **116**, 376-395.

BRACE, W. F. and KOHLSTEDT, D. L. (1980) Limits on lithospheric stress imposed by laboratory experiments: *Jour. Geophys. Res.* **85**, 6248-6252.

CARSLAW, H. S. and JAEGER, J. C. (1959) *Conduction of heat in solids*: Oxford, Clarendon Press, 510 p.

CHAPPLE, W. M. (1978) Mechanics of thin-skinned fold-and-thrust belts: *Geol. Soc. Amer. Bull.* **89**, 1189-1198.

CHEN, CHAO HSIA (1979) Geology of the east-west cross-island highway in central Taiwan: *Memoir Geol. Soc. China* **3**, 219-236.

CHEN, P. H., HUANG, C. Y., HUANG, T. C. and TSAI, L. P. (1977) A study of the late Neogene marine sediments of the Chishan area, Taiwan: paleomagnetic stratigraphy, biostratigraphy, and paleoclimate: *Memoir Geol. Soc. China* **2**, 169-190.

CHI, W. R., NAMSON, J. and SUPPE, J. (1981) Stratigraphic record of plate interactions in the Coastal Range of eastern Taiwan: *Memoir Geol. Soc. China* **4**, 155-194.

Chinese Petroleum Corporation (1971) *Geologic Map of Western Taiwan*: Taiwan Petroleum Exploration Division, Chinese Petroleum Corporation, Miaoli (Scale 1:200,000).

——— (1974) *Geologic Map of Western Taiwan, Miaoli Sheet*: Taiwan Petroleum Exploration Division, Chinese Petroleum Corporation, Miaoli (Scale 1:100,000).

——— (1978) *Geologic Map of Western Taiwan, Taoyuan-Hsinchu Sheet*: Taiwan Petroleum Exploration Division, Chinese Petroleum Corporation, Miaoli (Scale 1:100,000).

CLARK, S. P., JR. (1966) Handbook of physical constants: *Geol. Soc. America Memoir* **97**, 587 p.

DAVIS, D. M. and SUPPE, J. (1980) Critical taper in mechanics of fold-and-thrust belts: *Geol. Soc. America Abstracts w/Programs* **12**, 410.

HO, C. S. (1975) *An introduction to the geology of Taiwan—explanatory text of the geologic map of Taiwan*: Ministry of Economic Affairs, Republic of China, Taipei, 153 p.

(1979) Geologic and tectonic framework of Taiwan: *Memoir Geol. Soc. China* **3**, 57-72.

, Hsu, M. Y. and Jen, L. S. (1963) Fault structures in the Keelung coastal area, Taiwan: *Proc. Geol. Soc. China* **6**, 18-33.

and Fong, G. S. (1964) Geology and coal resources of the northern coastal area of Taiwan: *Bull. Geol. Survey Taiwan* **15**, 69 p.

Hoshino, K., Koide, H., Inami, K. Iwamura, S. and Mitsui, S. (1972) Mechanical properties of Japanese Tertiary sedimentary rocks under high confining pressures: *Geol. Survey Japan, Report* **244**, 200 p.

Hsu, T. L. (1956) Geology of the Coastal Range, eastern Taiwan: *Bull. Geol. Surv. Taiwan* **8**, 39-64.

(1976) The Lichi Melange in the Coastal Range framework: *Bull. Geol. Surv. Taiwan* **25**, 87-95.

Ku, T. L., Teng, T. L., Wu, T. M., Lee, Y. H., Wang, N. D., Yao, T. H., Hsu, L. C. and Juan, V. C. (1963) *Geologic Map of the Tatun Volcano Group and Its Adjacent Area, Taiwan*: National Taiwan University, Taipei (Scale 1:25,000).

Li, Y. H. (1975) Denudation of Taiwan island since the Pliocene Epoch: *Geology* **4**, 105-107.

Liou, J. G. (1981) Recent high CO_2 activity and Cenozoic progressive metamorphism in Taiwan: *Memoir Geol. Soc. China* **4**, 551-581.

McGarr, A. and Gay, N. C. (1978) State of stress in the Earth's crust: *Ann. Reviews Earth & Planetary Science*, **6** 405-436.

Page, B. M. and Suppe, J. (1981) The Pliocene Lichi Melange of Taiwan: its olistostromal and plate-tectonic origin: *Amer. Jour. Science* **281**, 193-227.

Peng, T. H., Li, Y. H. and Wu, F. T. (1977) Tectonic uplift rates of the Taiwan island since early Holocene: *Memoir Geol. Soc. China* **2**, 57-69.

Pytte, A. M. (1980) A study of abnormal pore-fluid pressures in Western Taiwan using sonic log: *unpublished Senior Thesis, Princenton University*, 69 p.

Seno, T. (1977) The instantaneous rotation vector of the Philippine Sea plate relative to the Eurasian plate: *Tectonophysics* **42**, 209-226.

Stanley, R. S. (1981) A cross section through the southern Central Mountains of Taiwan: *Memoir Geol. Soc. China* **4**.

Suppe, J. (1979) Fault-bend folding (abstract): *Geol. Soc. America Abstr. w/Programs* **11**, 525.

(1980a) A retrodeformable cross section of northern Taiwan: *Proc. Geol. Soc. China* **23**, 46-55.

(1980b) Imbricated structure of western foothills belt, south-central Taiwan: *Petroleum Geology Taiwan* **17**, 1-16.

, and Namson, J. (1979) Fault-bend origin of frontal folds of the western Taiwan fold-and-thrust belt: *Petroleum Geology Taiwan* **16**, 1-18.

, and Wittke, J. H. (1977) Abnormal pore-fluid pressures in relation to stratigraphy and structure in the active fold-and-thrust belt of northwestern Taiwan: *Petroleum Geology Taiwan* **14**, 11-24.

Thompson, J. B., Jr. (1955) The thermodynamic basis for the mineral facies concept: *Amer. Jour. Science* **253**, 65-103.

Tsai, Y. B., Teng, T. L., Chiu, J. M. and Liu, H. L. (1977) Tectonic implications of the seismicity in the Taiwan region: *Memoir Geol. Soc. China* **2**, 13-41.

Wang, Y. and Lee, C. M. W. (1981) Basement geology of Taiwan and some tectonic implications: *Seminar Plate Tectonics and Metamorphic Geology, Taipei, Abstract*, 54.

Wollenberg, H. A., Smith, A. R. and Bailey, E. H. (1967) Radioactivity of Upper Mesozoic graywackes in the northern Coast Ranges, California: *Jour. Geophysical Research* **72**, 4139-4150.

臺灣造山作用和變質作用之力學原理

蘇　　　　強

節　　　要

非律賓板塊以每百萬年七十公里的速率，以西北方向對著亞洲板塊移動 (Seno, 1977)。此運動造成呂宋火山島弧和中國大陸邊緣的斜向碰撞，同時使大陸邊緣之新生代沉積物形成臺灣島。碰撞是逐漸向南發展，其速率大約是每百萬年九十公里。因此初步估計在島弧或臺灣島上如要移動九十公里之遠，相當於時間上要退回一百萬年。利用此時空之對等關係，由臺灣南端向北移，我們可以知道陸核化的楔狀體（中央山脈）不斷上升，直到因造山運動而造成的物質增加量和因陵夷作用造成的物質流失量達到平衡時爲止。達到穩定狀態的山脈帶需經過約 1⅛ 百萬年，如其寬約九十公里，而其橫切面的增大爲每百萬年約五百平方公里。

在山脈地帶所受之壓縮，主要是由逆衝斷層滑動和底部脫卸構造上之楔型地塊受到斷層彎曲褶皺作用而引起。根據重建變形前區域剖面來推算，中國大陸邊緣受到逆衝斷層的影響，於臺灣北部至少縮短了一百五十至兩百公里。西部麓山帶中發生脫卸構造的主要地層因孔隙中流體壓力很高（大約是靜水壓的一點七倍），因此摩擦抗力低。有關山楔的力學原理，可以用一個「庫侖物質」構成的楔形體一直處於受擠壓被破壞的情形來說明，就好像是在推土機前面的楔形土堆一樣，它會一直變形，直到恰好達到穩定的表面 α 爲止。在一個厚 h 的楔形物體中，恰好在某點造成臨界錐形之情形，可以用下式表示 (Davis 和 Suppe, 1980)：

$$(\alpha+\beta)=\tan^{-1}=\left[\frac{(1-\lambda_f)(\sin\beta+\mu_f)}{\{\lambda_0+k_p(1-\lambda_0)\}+\{C_0(k_p-1)/(\rho gh\tan\phi)\}}\right]$$

上式中的 α 表示表面坡度，β 則是脫卸構造的傾斜角度。C_0 是內聚力，ϕ 是內摩擦係數，k_p = 〔$(1+\sin\phi)/(1-\sin\phi)$〕是被動地壓係數 (passive earth-pressure coefficient)，$\lambda_0=P_f/\rho gz$ 則是楔形體中的 Hubbert-Rubey 液壓率 (fluid-pressure ratio)，λ_f 和 μ_f 分別是流體壓力比值和沿脫卸構造底面的摩擦係數。在臺灣西部，我們直接測得 $\lambda_0=\lambda_f=0.7$，$\beta=6°$。$h<\backsim 4$ 公里，$0<\alpha<3°$，而 $h>\backsim 4$ 公里 $\alpha=3°$。根據 Byerlee 氏定律，$\mu_f=0.85$；獲得 $C_0\cong 5\,\mathrm{MPa}$ 及 $\phi\cong 30°$，這些數值和類似臺灣西部的沉積岩所測的岩石強度極爲相似。因此臺灣西部的變形山脈楔狀體具有和庫侖楔狀體一般的形狀。由山塊的區域成形可知道目前非塑性帶（在十至十三公里以上區域）的區域變質之物理情況，這些都和固體超壓力（固體壓力或平均應力 $\bar{\sigma}=1.3\bar{\rho}gz$）、流體壓力與固體壓力比值較低 ($P_f/\bar{\sigma}=0.5$) 有關。中國大陸邊緣在板塊碰撞之前的平均應力估計爲 $\bar{\sigma}=0.9\,\bar{e}gz$，並且具有較高的流體和固體壓力比值 $P_f/\bar{\sigma}=0.8$。由於板塊碰撞所造成的流體和固體壓力比值之下降，作者認是臺灣的區域變質作用發生在比十五公里淺的地方之重要原因。由石油探勘可知西部麓山帶之地溫梯度大約爲每公里上升攝氏三十五度。